FEBS openbio

FEBS PRESS science publishing by scientists

The β-domain of streptokinase affects several functionalities, including specific/proteolytic activity kinetics

Maryam Rafipour[1,2], Malihe Keramati[3], Mohammad Mehdi Aslani[2], Arash Arashkia[1] and Farzin Roohvand[1]

1 Virology Department, Pasteur Institute of Iran, Tehran, Iran
2 Microbiology Department, Pasteur Institute of Iran, Tehran, Iran
3 NanoBiotechnology Department, Pasteur Institute of Iran, Tehran, Iran

Keywords
fibrinolysis; plasminogen activation; protein domains; streptococci clusters; streptokinase; α2-antiplasmin resistance

Correspondence
F. Roohvand, Virology Department, Pasteur Institute of Iran, No. 69, Pasteur Ave., Tehran 1316943551, Iran
Fax/Tel: +98 21 66496682
E-mails: rfarzin@pasteur.ac.ir; farzin.roohvand@gmail.com

(Received 23 February 2019, revised 14 April 2019, accepted 13 May 2019)

doi:10.1002/2211-5463.12657

Streptokinase (SK) is a plasminogen activator which converts inactive plasminogen (Pg) to active plasmin (Pm), which cleaves fibrin clots. SK secreted by groups A, C, and G *Streptococcus* (SKA/SKC/SKG) is composed of three domains: SKα, SKβ and SKγ. Previous domain-swapping studies between SK1/SK2b-cluster variants revealed that SKβ plays a major role in the activation of human Pg. Here, we carried out domain-swapping between *skcg*-SK/SK2-cluster variants to determine the involvement of SKβ in several SK functionalities, including specific/proteolytic activity kinetics, fibrinogen-bound Pg activation and α_2-antiplasmin resistance. Our results indicate that SKβ has a minor to determining role in these diverse functionalities for *skcg*-SK and SK2b variants, which might potentially be accompanied by few critical residues acting as hot spots. Our findings enhance our understanding of the roles of SKβ and hot spots in different functional characteristics of SK clusters and may aid in the engineering of fibrin-specific variants of SK for breaking down blood clots with potentially higher efficacy and safety.

Streptokinase (SK), a plasminogen activator (PA) secreted by groups A, C and G streptococci (GAS, GCS and GGS, respectively), converts the inactive plasminogen (Pg) to the active plasmin (Pm) which cleaves the fibrin clots. Despite being considered as a virulence factor (especially in GAS pathogenesis), traditionally, a nonfibrin-specific SK, isolated from the less virulent GCS (H46A or ATCC9542), was widely used as a fibrinolytic drug [1,2]. PA activity of SK is accomplished in two pathways. First, it binds to Pg and forms a 1 : 1 binary SK-Pg* activator (amidolytic) complex, which converts the free Pg substrate to Pm (nonfibrin-specific pathway I). Subsequently, the generated Pm binds SK to form SK-Pm proteolytic activator complex which converts Pg molecules to Pm (fibrin-specific pathway II) [2,3].

The 414 amino acid, SK, is composed of three distinct structural domains: α, β and γ spanning residues: 1–146, 147–290 and 291–414, respectively. Protein engineering studies indicated the importance of all three domains and the potential role of several critical amino acids (hot spots), such as Ile1 [3], Lys256, Lys257 [4] and recently Ile33, Asn228 and Phe287 [5], for SK functionality. The attained information was used to improve the fibrinolytic characteristics of SK for enhanced PA potency, fibrin specificity and resistance to the inhibitory effect of plasma α_2-antiplasmin (α_2-AP). Concurrently, heterogeneity of SKs at the

Abbreviations
Fg, fibrinogen; PA, plasminogen activator; PAM, plasminogen-binding group A streptococcal M-like protein; Pg, plasminogen; Pm, plasmin; SA*, specific activity; SK, streptokinase; SKA/SKC/SKG, respectively, groups A, C and G *Streptococcus*; α_2-AP, alpha 2-antiplasmin.

 © 2019 The Authors. Published by FEBS Press and John Wiley & Sons Ltd.
This is an open access article under the terms of the Creative Commons Attribution License, which permits use, distribution and reproduction in any medium, provided the original work is properly cited.

gene (*sk*) and protein (SK) levels in different strains (even the same group) of streptococci (specifically for GAS) and its relation to functional differences was shown [2]. Studies indicated the highest sequence diversity of β-domain compared to α and γ, particularly in a distinct hypervariable region (*sk*-V_1; residues 147–218). Accordingly, the *sk*-V_1 was suggested as the main source of *sk* allelic variations, and consequently, phylogenetic analysis of the *sk*-V1 nucleotide sequences was used to classify the GAS-SK (*ska*) alleles into two main clusters; SK1 and SK2, in which SK2 was further subdivided into subclusters SK2a and SK2b [6,7]. These clusters successfully classified GAS strains into those that contain (a) a Pg/Pm direct binding M-like protein, 'PAM' and usually induce invasive skin infections (SK2b), (b) a fibrinogen (Fg) binding M1 protein that does not directly interact with Pg and usually induce upper respiratory tracts (UTR) infections (SK2a) and (c) a M protein that does not interact with either Pg or Fg (SK1) and optimally activates Pg in solution. Although presence of Fg generally enhances the PA activity of all SK types, the specific characteristic of SK1 for optimal Pg activation in solution is in contrast to the SK2 groups (specially SK2b) which strictly require the presence of Fg to display PA activity [6–9]. Interestingly, GCS/GGS-SKs (*skcg*), despite expressing Pg-binding proteins different from PAM and other GAS-M proteins and displaying high Pg activation in solution (similar to SK1), are clustered in SK2a section of the phylogenetic tree [6]. Indeed, most of the *ska* alleles in SK2a cluster are homologous to *skcg* than SK1 or SK2b. Moreover, complexes of Pm with SK2a and *skcg*-SK display higher resistance to inhibition by α_2-AP than SK1 or SK2b [1]. Therefore, *skcg*-SKs display some characteristics specific for either SK1 or SK2a clusters and are thus interesting candidates for comparative studies.

Attempts to address the role of β-domain heterogeneity for functional characteristics of SK clusters/subclusters started with a study on exchange and swapping the major polymorphic regions between SK1 β-domain (SK1β) and SK2aβ [10]. However, apparently due to the similar PA potencies of the used SK1 and SK2a variants, this study failed to uncover any effect on Pg activation kinetics of the chimeric and parental SKs. Recently, two other studies addressing the domain-exchange strategies between a SK1 (with high PA activation rate) and SK2b indicated the major role of the β-domain in the PA activity, which might be further assisted by α-domain [11]. But how β-domain exchange might alter the kinetics of the amidolytic/proteolytic pathways, Fg-bound-Pg activation or the resistance to inhibition by α_2-AP, specially between *skcg*-SK and SK2b, are other concerns that never addressed. Recently, SK from a newly isolated GGS (SKG88) with high PA activity was introduced [12]. In the present report, using SKG88 and two other SKs belonging to SK2a and SK2b and employing domain-exchange approaches, these concerns are addressed.

Materials and methods

Bacterial strains and reassessment of the SK clusters

The *skcg*-SK of GGS (G88) with high PA activities [12], which was supposed to be clustered as SK2a [6], was used for β-domain exchange between SK of two GAS strains; STAB902 containing SK2a with very low PA activities [13] and ALAB49 (gifted by Mc. Arthur, University of Wollongong, Australia), containing a well-known SK2b with barely detectable PA activities in culture supernatants [7]. The gene accession numbers are as follows: HM390000.1, CP007041.1 and AY234134, respectively. Sequence alignment and phylogenetic analysis of *sk*β-V1 region for these three SKs and six other well-known SK clusters [6,7] were accomplished by 'Molecular Evolutionary Genetics Analysis, MEGA6' [14].

Construction of the parental and β-domain-exchanged SK-encoding plasmids

The detailed steps for cloning of *sk* into pET26b vector to construct the parental plasmids (pET26b-SK_{G88}, pET26b-SK_{ALAB49} and pET26b-$SK_{STAB902}$) are illustrated in Fig. S2.

For construction of the β-domain-exchanged SKs, the region corresponding to nucleotides 375–699 (residues 125–233) from the parental vectors was digested by *BstE*II/*BsiW*I restriction enzymes and the digested fragments (327 bp) were cross ligated between SK_{G88} and two other SKs (SK_{ALAB49} and $SK_{STAB902}$) (Fig. 1B). All the molecular methods were based on the standard protocols [15].

Expression, purification and characterization of SK proteins

Escherichia coli Rosetta (Novagen, USA) was used for protein expression via IPTG induction, and expressed SKs were purified under native conditions using nickel-nitriloacetic acid (Ni-NTA) affinity chromatography (Qiagen, USA) according to the manufacturer's protocols (QIAexpressionist 2002; Qiagen). Protein concentrations were determined by Bradford assay. Expression and the purity of the purified SKs were assessed by 12% (w/v) SDS/PAGE and confirmed by western blotting. Protein characterizations assays are described in Figs S5 and S6.

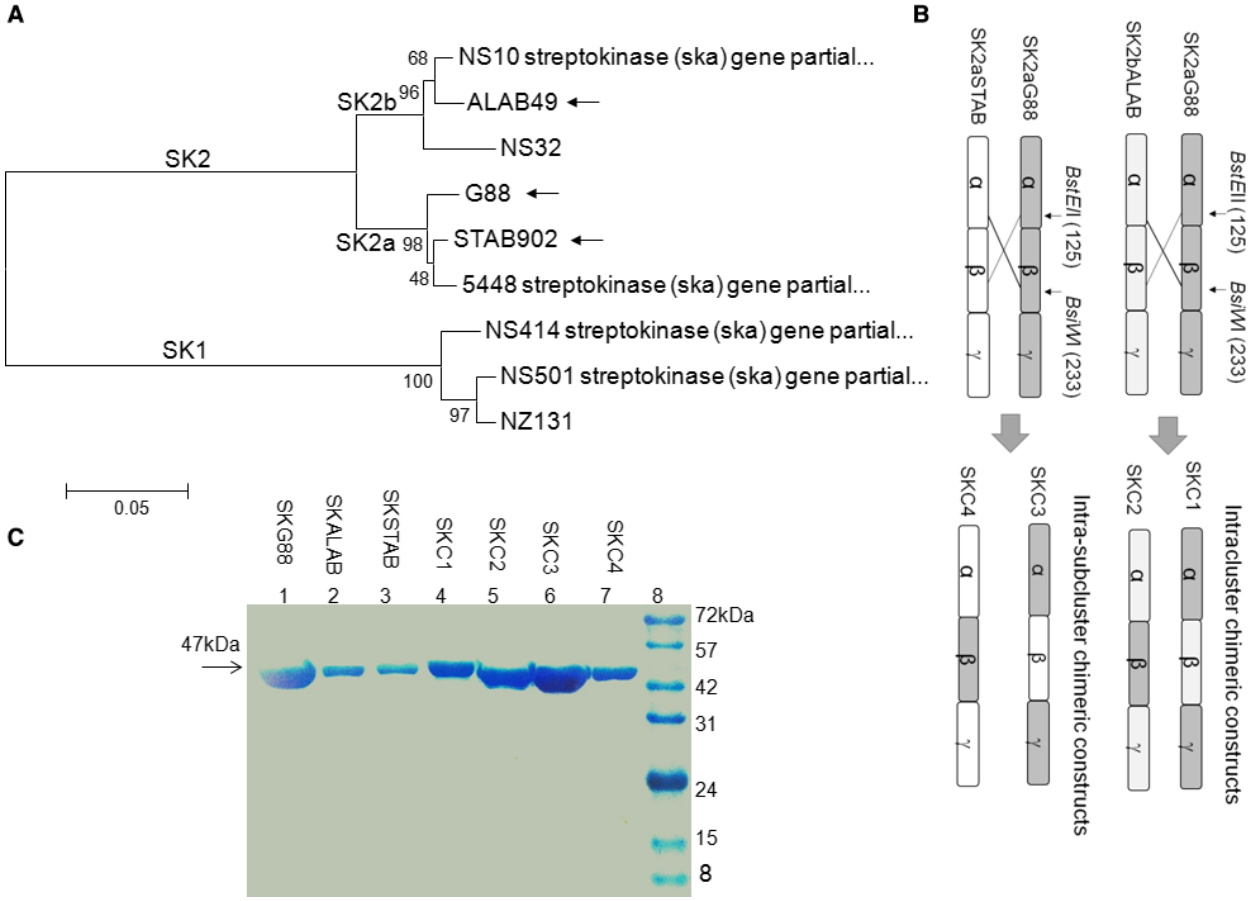

Fig. 1. Reassessment of the SK cluster, SKβ-exchange and analysis of the purified SKs. (A) Phylogenetic analysis on *sk*β-V1 region for three parental SKs (shown by arrows) and six other well-known SK clusters (NS10; EU352637.1, NS32; EU352630.1, 5448; CP008776.1, NS411; EU352621.1, NS501; EU352616.1, NZ131; CP000829.1) [6,7] was accomplished by 'Molecular Evolutionary Genetics Analysis, MEGA6' [14]. Bootstrap values of 90% (500 replicates) are indicated. Scale bar = 0.05 substitution per site. (B) Construction of chimeric SKs by β-domain exchange of residues 125–233 between parental SKs (the unique restriction sites used for sequence exchange are indicated). SK_{C1}/SK_{C2} and SK_{C3}/SK_{C4} were made by β-domain exchanges between $SK2a_{G88}$/$SK2b_{ALAB49}$ and $SK2a_{G88}$/$SK2a_{STAB902}$, respectively. (C) SDS/PAGE analysis of purified chimeric and parental SK proteins. Lanes 1–7: the purified SKs corresponding to each band were indicated above each well. Lane 8: molecular weight marker (SM7012, Cinnagen Co, Tehran, Iran).

Determination of SK-specific activity (SA*)

For evaluation of the SA* in the presence/absence of Fg, the standard colorimetric assay using the chromogenic substrate (S-2251; Sigma, USA) was used throughout this study, as previously described [7]. The detailed procedure for the assay, construction of the calibration curve and calculation of the SA* are provided in Fig. S7, Figs 2 and 3.

Determination of kinetic constants for amidolytic and proteolytic activities

For analysing amidolytic kinetics, first stoichiometric concentrations of Pg and SK (5.5 μM SK and 5 μM Pg) were mixed and incubated for 5 min to produce the SK-Pg* activator complex. Subsequently, an aliquot of the complex (100 nM) was transferred to the assay buffer along with various concentrations of S2251 (0.1–1.5 mM) in a total volume of 100 μL [12].

For analysing proteolytic kinetics, 100 nM of SK was added to assay buffer containing, '0.1 mM S2251 and varying concentrations of Pg (0.3–5.0 μM)' and changes in absorbance at 405 nm were monitored for 30 min. The data were plotted as velocity/substrate concentration, and kinetic parameters of Pg activation were determined from Michaelis–Menten (V vs S) and inverse ($1/V$ vs $1/S$) Lineweaver–Burk plots using GRAPHPAD PRISM 6 (GraphPad Software, La Jolla, CA, USA) [12].

Inhibition by α_2-antiplasmin

Stoichiometric complexes of SK-Pm (400 nM SK and 200 nM Pm) were incubated for 5 min. The complex was

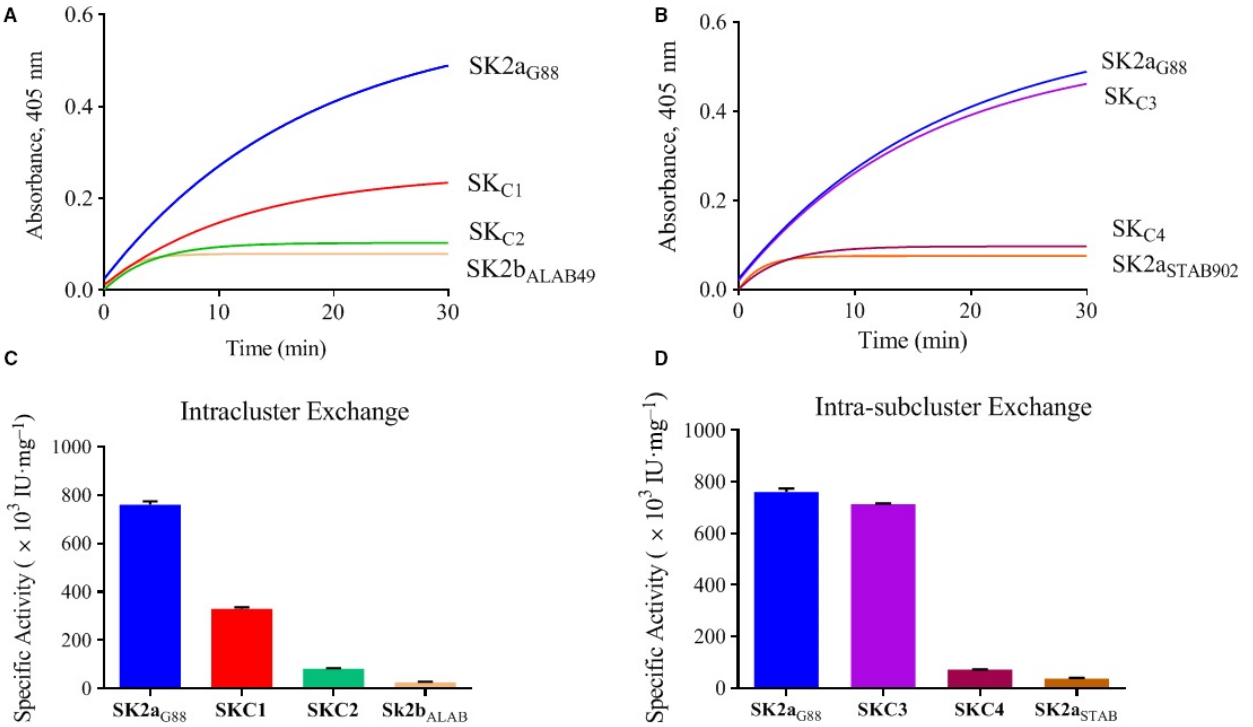

Fig. 2. Determination of PA activity of SKs by chromogenic assay using S-2251 substrate. The standard chromogenic assay by the synthetic chromogenic substrate, 'tripeptide H-D-valyl-L-leucyl-L-lysine-*p*-nitroanilide dihydrochloride (S-2251; Sigma)' which is an approved assay for determination of SK activity (Third International Standard for streptokinase; National Institute of Biological Standards and Controls, NIBSC, 2004UK), was used throughout the study. For determination of specific activities (SA*), purified SK proteins (100 nM) were added to a microtitre plate containing 1 mM of S-2251 and 1 μM of Pg (Sigma) in a total volume of 100 μL of assay buffer (50 mM Tris/HCl, pH 7.4). Hydrolysis of S-2251 was measured at 405 nm every 5 min for 60 min in a microplate reader (Synergy™ 4, BioTek-Fisher Scientific, UK). All reactions were performed in triplicate. Serial dilutions of Streptase® (CSL, Behring, Germany), a commercially available standard SK, were used to prepare the standard calibration curve (Fig. S7) which was needed for calculating SK-specific activities (SA*). For calculation of the SA*, the time-course activity profiles (the change in absorbance at 405 nm as a function of time) were measured (Fig. 2A,B), and subsequently, SA* (Fig. 2C,D) was calculated from the slope of the linear portion of the curve (Fig. 3) in which serial dilutions of commercial (standard) SK (Streptase) were used as the reference for calibration (Fig. S7). SK2a$_{G88}$, SK2b$_{ALAB49}$ and SK2a$_{STAB902}$ are parental constructs. SK$_{C1}$ (2a$_{G88}$-2b$_{ALAB}$-2a$_{G88}$) and SK$_{C2}$ (2b$_{ALAB}$-2a$_{G88}$-2b$_{ALAB}$) denote the intracluster chimeras. SK$_{C3}$ (2a$_{G88}$-2a$_{STAB}$-2a$_{G88}$) and SK$_{C4}$ (2a$_{STAB}$-2a$_{G88}$-2a$_{STAB}$) denote the intra-subcluster chimeras. Data represent the mean ± SD of triplicate experiments.

diluted to 20 nM in assay buffer containing α_2-AP (final concentration: 100–400 nM). The mixtures were incubated for 15 min, then S-2251 (500 μM) was added to the reaction, and residual activity of complex was measured by change in absorbance at 405 nm [1].

Statistical analyses

Unpaired, two-tailed Student's *t* test with 95% confidence intervals was used for analysis of SK-PA activities and kinetics using SPSS software version 22.0 (SPSS Inc., USA). All linear regressions were by GRAPHPAD PRISM 6, and *P*-values < 0.05 were considered significant.

Results and Discussion

Confirmation of the SK clusters and production of SK proteins

Sequence alignment of *sk*β-V1 region for G88, STAB902 and ALAB49 and six other well-known SK clusters [6,7] that were used for construction of the phylogenetic tree is provided in Fig. S1. Phylogenetic analysis (Fig. 1A) identified the *skg*-encoded-SKG88 as SK2a (SK2a$_{G88}$) which is in complete agreement with prior reports on clustering of *skcg* alleles [6]. Accordingly, STAB902 and ALAB49 SKs were

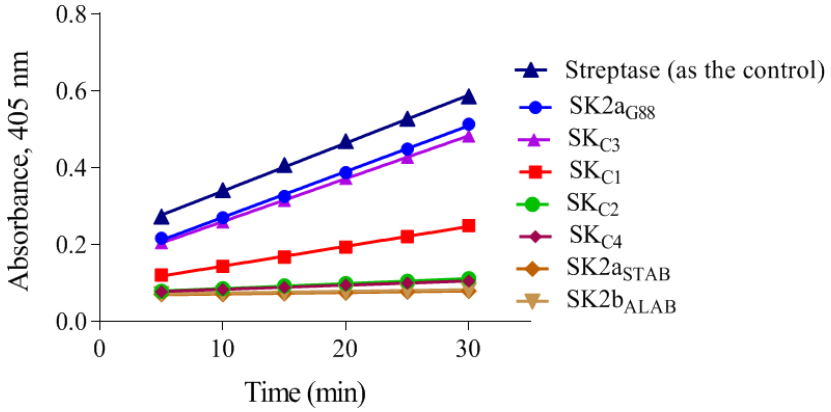

Fig. 3. The time-course activity profiles (the change in absorbance at 405 nm as a function of time) of SKs. For measuring the specific activity (IU·mg^{-1}) of the SKs, the slopes of the linear portion of the curve obtained from plotting absorbance (OD) at 405 nm vs time (Fig. 2A,B) were used. Serial dilutions of Streptase® (CSL) were used as reference for preparation of the standard curve (Fig. S7) and calibration of international units·mg^{-1} protein (specific activity) in the samples. SK2a$_{G88}$, SK2b$_{ALAB49}$ and SK2a$_{STAB902}$ are parental constructs. SK$_{C1}$ (2a$_{G88}$-2b$_{ALAB}$-2a$_{G88}$) and SK$_{C2}$ (2b$_{ALAB}$-2a$_{G88}$-2b$_{ALAB}$) denote the intracluster chimeras. SK$_{C3}$ (2a$_{G88}$-2a$_{STAB}$-2a$_{G88}$) and SK$_{C4}$ (2a$_{STAB}$-2a$_{G88}$-2a$_{STAB}$) denote the intra-subcluster chimeras.

subclustered as SK2a (SK2a$_{STAB902}$) and SK2b (SK2b$_{ALAB49}$), respectively [7,13]. PCR amplification of all three parental SKs produced the expected 1250-bp amplicon (Fig. S3). Cloning steps for insertion of parental SKs (SK2a$_{G88}$, SK2b$_{ALAB49}$, SK2a$_{STAB902}$) into pET26b vector and exchange of the 327-bp β-domain (*BstE*II/*BsiW*I) fragments between SK2a$_{G88}$ and SK2b$_{ALAB49}$ (hereafter intracluster chimeric constructs; SK$_{C1}$ and SK$_{C2}$) and between SK2a$_{G88}$ and SK2a$_{STAB902}$ (hereafter intra-subcluster chimeric constructs; SK$_{C3}$ and SK$_{C4}$) vectors are illustrated in Fig. S2 and Fig. 1B, respectively. Restriction analyses of the recombinant SK-encoding vectors (Fig. S4) and nucleotide sequence analysis (Fig. S8) confirmed the accuracy of the cloning procedures. Characterization of the expressed SK proteins by SDS/PAGE (Fig. S5A) and western blotting (Fig. S6), in accordance with the prior reports [11,12,16], indicated the expression of SKs with the expected size (47 kDa). Purification by one-step Ni-NTA affinity chromatography resulted in 90% purity (Fig. 1C and Fig. S5B).

Contribution of the SKβ in specific activity (SA*)

For calculation of the SA*, the time-course activity profiles (the change in absorbance at 405 nm as a function of time) were measured (Fig. 2A,B), and subsequently, SA* was calculated (Fig. 2C,D and Table 1), from the slope of the linear portion of the curve (Fig. 3) in which serial dilutions of commercial/standard SK (Streptase) were used as the reference for calibration (Fig. S7). As shown in Table 1, the SA* of SK2a$_{G88}$ (760.82×10^3 IU·mg^{-1}) was about 28-fold and 22-fold higher than that of SK2b$_{ALAB49}$ (26.64×10^3 IU·mg^{-1}) and SK2a$_{STAB902}$ (36.50×10^3 IU·mg^{-1}), respectively. Prior studies reported over 10-fold higher PA activity for SK1 compared to SK2b [8,11] which further supports the similarity of SK1 and *skcg*-SK (SK2a$_{G88}$) for optimal PA activity in solution [11]. Indeed, SK1β is the most divergent among all SK clusters, and the divergence between SK1 and SK2b might even exceed 40% [6,7], which might further support the determining role of β-domain for functional characteristics between SK1 and SK2b clusters [11,16]. But sequence alignments (Fig. S8 and Table 3) indicated that the exchanged β-domains between SK2a$_{G88}$ and SK2b$_{ALAB49}$ (intracluster; Fig. 1B) were 89% similar, while α- and γ-domains exhibited 82% and 86% similarity, respectively. Therefore α- and γ-domains might have more contribution in functional characteristics of the *skcg*/SK2b domain-exchanged SKs in our study (SK$_{C1}$/SK$_{C2}$) than that of SK1/SK2b in the prior report [11]. In contrast, exchanging the SK2a$_{G88}$β and SK2a$_{STAB902}$β, for making the two intra-subcluster constructs (SK$_{C3}$; 2a$_{G88}$-2a$_{STAB}$-2a$_{G88}$ and SK$_{C4}$; 2a$_{STAB}$-2a$_{G88}$-2a$_{STAB}$; Fig. 1B) led to less alterations in the SA* values for SK$_{C3}$/SK$_{C4}$ compared to SK2a$_{G88}$ and SK2b$_{ALAB49}$ (Fig. 2D and Table 1). Thus, our results, consistent with a prior study on SK1β and SK2aβ exchanged domains, could not uncover any major effects on PA potencies [10]. However, in the prior study, despite sharing less than 50% identity between exchanged SK1β

and SK2aβ, the parental SKs had relatively similar SA* [10], while despite clustering as SK2a, the $SK2a_{G88}$ and $SK2a_{STAB902}$ in our study show highly different SA* (Table 1). Indeed, the exchanged β-domains (residues 128–233) of $SK2a_{G88}$ and $SK2a_{STAB902}$ were around 97% identical (corresponding to only three residue substitutions out of 108; K138S, I151V, E161K; Table 3) while their α- and γ-domains exhibited 85% and 88% similarity, respectively (Fig. S8). Therefore, it might be the presence of only few scattered residues acting as hot spots rather than accumulated altered residues in a specific domain that counts for the highly different SA* activities, as recently claimed [5]. Having shown that β-domain exchange between SK2a intra-subclusters (SK_{C3}/SK_{C4}) had little contribution to SA*, the rest of the experiments were only performed for SK_{C1}/SK_{C2}.

Contribution of the SKβ in the kinetics of amidolytic/proteolytic activity

Amidolytic/proteolytic activity of the SKs was studied by measuring the steady-state kinetic constants of the S2251 hydrolysis including substrate affinity (K_m), catalytic activity (K_{cat}) and the constant of catalytic efficiency (K_{cat}/K_m; efficiency of the Pg conversion into Pm). As shown in Table 2, K_m and K_{cat} values did not alter significantly between SK_{C1} and $SK2a_{G88}$ (0.39 mM and 1.39 s^{-1} vs 0.41 mM and 1.39 s^{-1}, respectively) leading to almost similar catalytic efficiency (K_{cat}/K_m). For SK_{C2} compared to $SK2b_{ALAB49}$, the K_{cat} raised by 2.5% (0.88 vs 0.86 s^{-1}) and the K_m reduced by 17% (0.34 vs 0.41 mM) leading to an overall 24% increase in catalytic efficiency (2.59×10^3 vs 2.10×10^3 $s^{-1}\cdot M^{-1}$) (Table 2). Interestingly, evaluation of the kinetic parameters for proteolytic activity indicated that the catalytic efficiency of SK_{C1} declined by 47% compared to $SK2a_{G88}$ (229.27×10^3 vs 428.57×10^3 $s^{-1}\cdot M^{-1}$), which was mainly due to threefold increase in K_m value (0.77 vs 2.05 μM). For SK_{C2} compared to $SK2b_{ALAB49}$, the K_m declined by 57% (3.45 vs 7.92 μM) and the K_{cat} increased by 40% (0.22 vs 0.16 s^{-1}) leading to more than threefold augmented values for catalytic efficiency (63.77×10^3 vs 20.20×10^3 $s^{-1}\cdot M^{-1}$). These results indicated the determining role of the *skcg*β ($SK2a_{G88}$β) on enhancement of proteolytic activity (Table 2), mainly due to the augmentation of the K_m values (increased substrate affinity) which is in accordance with the SA* results (Table 1). Our results are consistent with a prior report on the importance of the SKβ for strong binding of Pg substrate to the SK-Pm proteolytic complex and its efficient conversion to Pm [17].

Contribution of the SKβ on Fg-bound-Pg activation

The Pg activation rate of various SKs in the presence/absence of Fg was measured by monitoring the absorbance at 450 nm and calculated by linear regression

Table 1. Specific activities of SK variants.

Parental SK[a]	Specific activity ($\times 10^3$ IU·mg^{-1})	Chimeric SK[a]		Specific activity ($\times 10^3$ IU·mg^{-1})
$SK2a_{G88}$ (α2aβ2aγ2a)	760.82 ± 13.63	Intracluster	SK_{C1} ($2a_{G88}$-$2b_{ALAB}$-$2a_{G88}$)	329.24 ± 7.07
$SK2b_{ALAB49}$ (α2bβ2bγ2b)	26.64 ± 1.79		SK_{C2} ($2b_{ALAB}$-$2a_{G88}$-$2b_{ALAB}$)	83.24 ± 1.28
$SK2a_{STAB902}$ (α2aβ2aγ2a)	36.50 ± 1.02	Intra-subcluster	SK_{C3} ($2a_{G88}$-$2a_{STAB}$-$2a_{G88}$)	713.54 ± 2.64
			SK_{C4} ($2a_{STAB}$-$2a_{G88}$-$2a_{STAB}$)	70.84 ± 0.89

All measured *P*-values were less than 0.05 ($P < 0.05$) considered significant.
[a]Parental and chimeric SK denote the three originally isolated SKs and four SKβ-exchanged SKs. Please see the text for complete explanations.

Table 2. Kinetic parameters for amidolytic/proteolytic activities of SK variants.

	Amidolytic constants			Proteolytic constants		
SK variants	$K_m \times 10^{-3}$ (M)	K_{cat} (s^{-1})	$K_{cat}/K_m \times 10^3$ ($s^{-1}\cdot M^{-1}$)	$K_m \times 10^{-6}$ (M)	K_{cat} (s^{-1})	$K_{cat}/K_m \times 10^3$ ($s^{-1}\cdot M^{-1}$)
$SK2a_{G88}$	0.41 ± 0.006	1.39 ± 0.031	3.39	0.77 ± 0.14	0.33 ± 0.082	428.57
$SK2b_{ALAB49}$	0.41 ± 0.048	0.86 ± 0.122	2.10	7.92 ± 0.16	0.16 ± 0.004	20.20
SK_{C1}	0.39 ± 0.062	1.39 ± 0.092	3.56	2.05 ± 0.753	0.47 ± 0.237	229.27
SK_{C2}	0.34 ± 0.052	0.88 ± 0.090	2.59	3.45 ± 0.23	0.22 ± 0.018	63.77

All measured *P*-values were less than 0.05 ($P < 0.05$) considered significant.

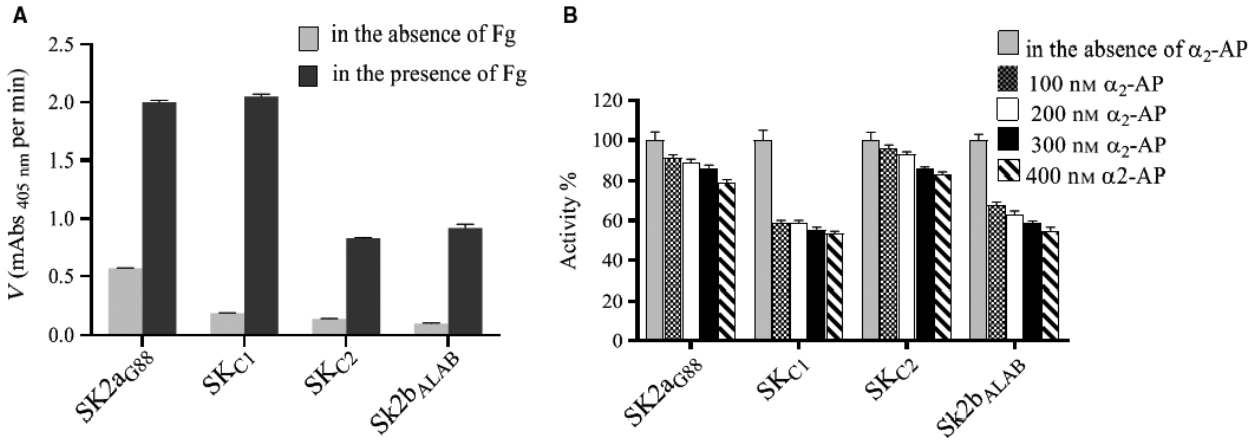

Fig. 4. Comparison the activity of SK variants in the absence/presence of (A) fibrinogen (Fg) or (B) α_2-antiplasmin (α_2-AP) (A) Measurement of SK activity in the presence of Fg was also based on hydrolysis of S-2251 by Pg. Fg (1 μM) and Pg (1 μM) were mixed (1 : 1 stoichiometric ratio) and pre-incubated for 15 min. Subsequently, SK (100 nM) and S-2251 (1 mM) were added to the mixture. The hPg activation rate of various SKs in presence and absence of Fg was measured by monitoring the absorbance at 450 nm and calculated by linear regression from the linear regions of plots A405 nm vs time (Fig. 5). The activation rate of all constructs belonging to either SK2a or SK2b cluster improved several orders of magnitude ranging from 3.5-fold in case of SK2a$_{G88}$ to 10.8-fold in case of SK$_{C1}$ in the presence of hFg. Notably, Fg stimulates the activity of cluster 2b more efficiently than that of cluster 2a. (B) The inhibitory effect of α_2-AP on SK-hPn complex activity in different concentrations of the inhibitor was illustrated relative (%) to the activity of the complex in absence of the inhibitor. Stoichiometric complexes of SK-hPn (20 nM) were performed for 5 min at 37 °C and incubated for 15 min at 37 °C with α_2-AP (final concentration 100–400 nM). The reactions were initiated by addition of S-2251 (500 mM) to complex mixtures, and the activity of the SK-hPn complexes was determined by measuring the absorbance at 405 nm. All SK-hPn complexes resisted the inhibitory effect of α_2-AP, but to different degrees, SK2a retained more than 80% of the activity in presence of the maximum concentration of α_2-AP, whereas SK2b residual activity in the highest concentrations of the inhibitor was almost 50%. SK$_{C1}$ (2a$_{G88}$-2b$_{ALAB}$-2a$_{G88}$) and SK$_{C2}$ (2b$_{ALAB}$-2a$_{G88}$-2b$_{ALAB}$) are the intracluster β-domain-exchanged variants; SK2a$_{G88}$ and SK2b$_{ALAB49}$ are the parental SKs. Data represent the mean ± SD of triplicate experiments. All measured *P*-values were less than 0.05 ($P < 0.05$) considered significant.

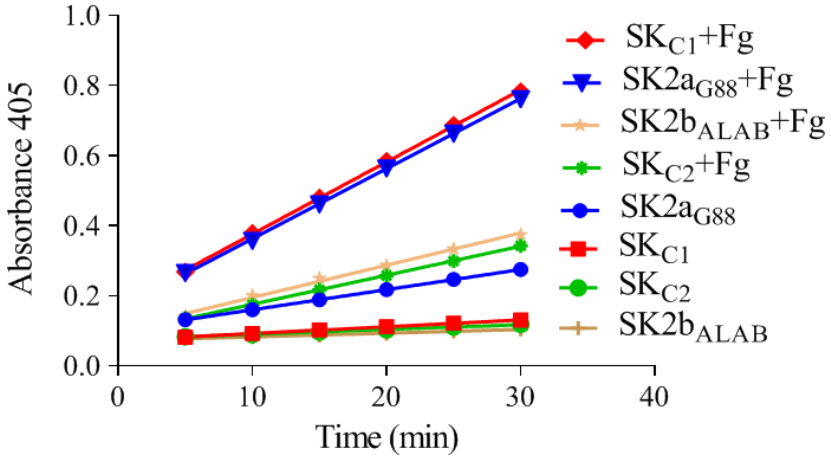

Fig. 5. The time-course activity profiles (the change in absorbance at 405 nm as a function of time) of SKs, in the presence/absence of fibrinogen (Fg). The Pg activation rates were measured by monitoring the absorbance at 450 nm and calculated by linear regression from the linear regions of plots A405 nm vs time. In the presence of Fg, activation rate (ΔOD405/t) of all SKs raised significantly but the effect is more reflective for SK2bβ containing constructs (SK$_{C1}$ and SK2b$_{ALAB49}$). SK2aG88 and SK2b$_{ALAB49}$ are parental constructs. SK$_{C1}$ (2a$_{G88}$-2b$_{ALAB}$-2a$_{G88}$) and SK$_{C2}$ (2b$_{ALAB}$-2a$_{G88}$-2b$_{ALAB}$) denote the intracluster chimeras.

from the linear regions of the plots (OD$_{405}$/time). As shown in Figs 4A and 5, generally, in the presence of Fg, activation rate (ΔOD$_{405}$/t) of all SKs (SK2a$_{G88}$, SK$_{C1}$, SK$_{C2}$, SK2b$_{ALAB49}$) raised significantly (2.00, 2.00, 0.83, 0.92×10^{-2} vs 0.57, 0.19, 0.14, 0.10×10^{-2}, respectively), but the effect is more

Table 3. The altered residues in the exchanged SKβ domain of $SK2a_{G88}$ compared to $SK2a_{STAB902}$ and $SK2b_{ALAB49}$. Conserved (identical) residues are indicated by dots.

	Residue position												
SK variant	132	134	138	151	153	154	160	161	176	178	209	210	213
$SK2a_{G88}$	V	E	K	I	N	Q	V	E	R	G	K	T	G
$SK2a_{STAB902}$	.	.	S	V	.	.	.	K	.	.	.	.	.
$SK2b_{ALAB49}$	I	Q	R	.	T	P	I	R	K	V	E	S	D

reflective for SK2bβ containing constructs (SK_{C1}/$SK2b_{ALAB49}$) than $SK2a_{G88}$/SK_{C2} (10.80/9.20 vs 3.51/5.93-fold enhancement of activation rates, respectively). These results are consistent with prior reports for higher influence of Fg on enhancement of SK2b activity compared to SK1 [7,8] and that of the SK2a compared to a *skc*-SK [9], indicating more similarity of the *skcg* ($SK2a_{G88}$) to SK1 variants for activation of Fg-bound-Pm. As shown in Fig. 4A and consistent with a recent study [12], $SK2a_{G88}$ showed high intrinsic Fg-bound-Pg activation. This higher Fg-bound-Pg activation (twofold higher than $SK2b_{ALAB49}$; 2.00 vs 0.92) is completely retained in SK_{C1}, while in the absence of Fg, PA potency of SK_{C1} is three times lower than the parental $SK2a_{G88}$ (0.19 vs 0.57). Of note, these characteristics of SK_{C1} might be of interest for development of a fibrin-specific version of SK for targeted fibrinolysis [3]. Interestingly, SK_{C2} retained the same (and low) activity as $SK2b_{ALAB49}$ in the absence of Fg, while its Fg-bound-Pg activation showed 42% (0.83 vs 2.00) and 90% (0.83 vs 0.92) of the parental activity ($SK2a_{G88}$ and $SK2b_{ALAB49}$, respectively). Collectively, while these results support the major contribution of the SKβ for the Fg-bound-Pg, but in agreement with prior reports also implies the potential contribution of other domains for this characteristic [3].

Contribution of the SKβ on resistance to α_2-AP inhibition

As shown in Fig. 4B, all four SK-Pm complexes resisted the inhibitory effect of α_2-AP (400 nM) by retaining more than 50% of their activity. This observation is consistent with the long-known phenomena for resistance of the SK-Pm complex to the major physiological plasmin inhibitor 'α_2-AP' [18]. However, for $SK2a_{G88}$ and SK_{C2} (containing $SK2a_{G88}$β), retained activity was about 80%, while for that of $SK2b_{ALAB49}$ and SK_{C1} (containing $SK2b_{ALAB49}$.β), it was about 50% (Fig. 4B). Thus, our results indicated that *skcg*-SK was more resistant to inhibition by α_2-AP than SK2b, which is in agreement with recent findings for Pm-complexed with either SK-H46A (*skc*) or SK2a variants [1]. Therefore, our results indicated the resemblance of *skcg*-SK to SK2a variants for 'α_2-AP resistance' and the determining role of SKβ in these characteristic. Although this finding is consistent with prior suggestion on the contribution of SKβ to the interaction of SK with inhibitors [19], the role of other domains, specially residue 1–59 of α-domain for resistance to α_2-AP, was also suggested [3].

Potential contribution of the substituted residues (hot spots) in SK functionalities

As emphasized earlier, a recent study on a new isolate of *skcg*-SK (GGS-132) indicated that presence of only three altered residues (Ile33Phe, Asn228Lys and Phe287Ile) that probably acted in a synergic mode as hot spots might induce enhanced proteolytic/Fg-bound-Pg activation compared to a SKC (GCS-SKC9542) [5,12]. Accordingly, it was also shown that $SK2a_{G88}$, in the present study, exhibited enhanced proteolytic/Fg-bound-Pg activation compared to the same SKC, while only seven residues scattered within domains of the two SKs were substituted (98% similarity) [12]. As shown in Table 3, the exchanged segments between $SK2a_{G88}$β and $SK2b_{ALAB49}$β differ by 12 residues. Among these altered residues, 'V160I, E161R and K209E', consistent with a recent report [17], might have potentially acted as hot spots for the induced functionalities of the domain-swapped SKs (SK_{C1}/SK_{C2}). The precise insight on the effect of these substitutions might be gained via site-directed mutagenesis experiments.

In conclusion, to the best of our knowledge, we reported the first domain-exchange study for *skcg* and cluster 2-*ska* alleles to elucidate the contribution of SKβ for a broad range of functional characteristic including kinetics of specific/ proteolytic activity, fibrinogen-bound Pg activation and α_2-antiplasmin resistance. Results pointed to the 'minor to determining' contribution of SKβ in these functionalities which might be potentially accompanied by a few critical residues acting as hot spots. Our findings indicated the (a) similarity of coclustered, *skcg*β and SK2aβ

variants (only three residues alteration) and minor contribution of their SKβ for highly different SA* between these two alleles; (b) similarity of *skcg to* cluster 1-*ska* alleles (SK1) for optimal PA activity in solution and activation of Fg-bound-Pm compared to that of the SK2 variants and major contribution of SKβ in this characteristic; (c) major role of the SKβ on enhancement of proteolytic activity between *skcg*-SK and SK2b that is mainly due to the augmentation of the K_m values (increased substrate affinity); and (d) similarity of *skcg*-SK *to* SK2a variants for 'α_2-AP resistance' and the determining role of SKβ in this characteristics. These findings might assist in better understanding of the roles displayed by SKβ and hot spots for different functional characteristic of SK clusters and engineering fibrin-specific versions of SK.

Acknowledgements

This study was financially supported by Pasteur Institute of Iran (BP-8922) in partial fulfilment of the Ph.D thesis of MR in medical biotechnology programme.

Conflict of interest

The authors declare no conflict of interest.

Author contributions

MR, the Ph.D candidate, did most of the experiments and prepared the primary draft of the manuscript. MK, the 1st advisor, assisted in cloning and kinetics analysis and design of the study. MMA, the 2nd supervisor, assisted in strain isolation and microbiology assays, and design of the study. AA, the 2nd advisor, assisted in protein expression and purification assays. FR, the 1st supervisor, designed and supervised the study and prepared the final manuscript for submission.

References

1 Cook SM, Skora A, Gillen CM, Walker MJ and McArthur JD (2012) Streptokinase variants from *Streptococcus pyogenes* isolates display altered plasminogen activation characteristics–implications for pathogenesis. *Mol Microbiol* **86**, 1052–1062.

2 Keramati M, Arabi Mianroodi R, Memarnejadian A, Mirzaie A, Sazvari S, Aslani MM and Roohvand F (2013) Towards a superior streptokinase for fibrinolytic therapy of vascular thrombosis. *Cardiovasc Hematol Agents Med Chem* **11**, 218–229.

3 Sazonova IY, McNamee RA, Houng A, King S, Hedstrom L and Reed GL (2009) Reprogrammed streptokinases develop fibrin-targeting and dissolve blood clots with more potency than tissue plasminogen activator. *J Thromb Haemost* **7**, 1321–1328.

4 Chaudhary A, Vasudha S, Rajagopal K, Komath SS, Garg N, Yadav M, Mande SC and Sahni G (1999) Function of the central domain of streptokinase in substrate plasminogen docking and processing revealed by site-directed mutagenesis. *Protein Sci* **8**, 2791–2805.

5 Kazemi F, Arab SS, Mohajel N, Keramati M, Niknam N, Aslani MM and Roohvand F (2018) Computational simulations assessment of mutations impact on streptokinase (SK) from a group G streptococci with enhanced activity–insights into the functional roles of structural dynamics flexibility of SK and stabilization of SK–μplasmin catalytic complex. *J Biomol Struct Dyn* **37**, 1944–1955.

6 Kalia A and Bessen DE (2004) Natural selection and evolution of streptococcal virulence genes involved in tissue-specific adaptations. *J Bacteriol* **186**, 110–121.

7 McArthur JD, McKay FC, Ramachandran V, Shyam P, Cork AJ, Sanderson-Smith ML, Cole JN, Ringdahl U, Sjobring U and Ranson M (2008) Allelic variants of streptokinase from *Streptococcus pyogenes* display functional differences in plasminogen activation. *FASEB J* **22**, 3146–3153.

8 Zhang Y, Liang Z, Hsueh HT, Ploplis VA and Castellino FJ (2012) Characterization of streptokinases from group A streptococci reveals a strong functional relationship that supports the coinheritance of plasminogen-binding M protein and cluster 2b streptokinase. *J Biol Chem* **287**, 42093–42103.

9 Huish S, Thelwell C and Longstaff C (2017) Activity regulation by fibrinogen and fibrin of streptokinase from *Streptococcus pyogenes*. *PLoS ONE* **12**, e0170936.

10 Lizano S and Johnston KH (2005) Structural diversity of streptokinase and activation of human plasminogen. *Infect Immun* **73**, 4451–4453.

11 Zhang Y, Liang Z, Glinton K, Ploplis VA and Castellino FJ (2013) Functional differences between *Streptococcus pyogenes* cluster 1 and cluster 2b streptokinases are determined by their β-domains. *FEBS Lett* **587**, 1304–1309.

12 Keramati M, Aslani MM, Khatami S and Roohvand F (2017) Sequence and kinetic analyses of streptokinase from two group G streptococci with high fibrin-dependent plasminogen activities and the identification of novel altered amino acids as potential hot spots. *Biotechnol Lett* **39**, 889–895.

13 Soriano N, Vincent P, Moullec S, Meygret A, Lagente V, Kayal S and Faili A (2014) Closed genome sequence of noninvasive *Streptococcus pyogenes* M/emm3 strain STAB902. *Genome Announc* **2**, e00792–e00814.

14 Tamura K, Stecher G and Peterson D (2013) MEGA6: molecular evolutionary genetics analysis (MEGA) software version 6.0. *Mol Biol Evol* **30**, 2725–2729.
15 Sambrook J and Russell DW (2006) *The Condensed Protocols from Molecular Cloning: A Laboratory Manual*, pp. 1957. Cold Spring Harbor Laboratory Press, Cold Spring Harbor, NY.
16 Zhang Y, Mayfield JA, Ploplis VA and Castellino FJ (2014) The β-domain of cluster 2b streptokinase is a major determinant for the regulation of its plasminogen activation activity by cellular plasminogen receptors. *Biochem Biophys Res Commun* **444**, 595–598.
17 Tharp AC, Laha M, Panizzi P, Thompson MW, Fuentes-Prior P and Bock PE (2009) Plasminogen substrate recognition by the streptokinase-plasminogen catalytic complex is facilitated by Arg253, Lys256, and Lys257 in the streptokinase beta-domain and kringle 5 of the substrate. *J Biol Chem* **284**, 19511–19521.
18 Cederholm-Williams SA, De Cock F, LijnenHR and CollenD (1979) Kinetics of the reactions between streptokinase, plasmin and α_2-antiplasmin. *Eur J Biochem* **100**, 125–132.
19 Gladysheva IP, Sazonova IY, Chowdhry SA, Liu L, Turner RB and Reed GL (2002) Chimerism reveals a role for the streptokinase β-domain in nonproteolytic active site formation, substrate, and inhibitor interactions. *J Biol Chem* **277**, 26846–26851.

Supporting information

Additional supporting information may be found online in the Supporting Information section at the end of the article.

Fig. S1. Multiple DNA Sequence alignment of *skβ*-V1 fragments. Multiple Sequence alignment of skβ-V1 fragments (hypervariable region1 of the β-domain)from nucleotide "445 to 655" of *sk* gene, corresponding to the amino acid residues "147 to 218" of the SK of the strains used in this study (G88, STAB902 and ALAB49; Genbank Accession numbers: HM390000.1, CP007041.1 and AY234134, respectively) together with the well-known strains that were employed for construction of phylogenetic tree in Fig. 1A (Genbank Accession numbers: NS10; EU352637.1, NS32; EU352630.1, 5448; CP008776.1, NS414; EU352621.1, NS501; EU352616.1, NZ131; CP000829.1). The alignment was created using MEGA software [14]. Conserved (identical) nucleotides are indicated by dots.

Fig. S2. Schematic illustration for construction of the parental SK-encoding plasmids. For construction of the three parental constructs, the genomic DNA from culture of the three targeted streptococci (G88, STAB902 and ALAB49) grown in BHI (brain heart infusion) broth, were isolated by DNA extraction kit (Qiagen, USA) according to the manufacturer's protocols. The extracted genomic DNA was used as template for PCR-based amplification of the coding region of *sk* genes (lacking the signal peptide sequence) using a pair of primers with inserted restriction sites (*Nde*I-*Xho*I) for direct cloning into pET26b vector (forward primer; *Nde*I-SKf: 5′-GACGAGACATATGATTGCT GGACCTGAGTG-3′; reverse primer; *Xho*I-SKr 5′-GA CACTCGAGTTTGTCGTTAGGGTTATCAG-3′, the sequences corresponding to restriction sites are underlined). The resulting amplified fragments were digested with *Nde*I and *Xho*I and cloned into the same sites of pET26b expression vector downstream of T7 promoter, in tandem with the fused C-terminus 6XHis-tag to provide the three parental SK-encoding vectors (pET26b-SK_{G88}, pET26b-SK_{ALAB49} and pET26b-$SK_{STAB902}$). All cloning steps were performed according to standard procedures [15]. ATG stands for vector-derived, translation-start codon; MCS, multiple cloning sites; 6His-tag is the tag derived from the vector.

Fig. S3. Analysis of the PCR-amplified *sk* genes by agarose gel (1%) electrophoresis. The coding region of *sk* gene (lacking the signal peptide sequence) was amplified by PCR using SKf and SKr primers. PCR reactions resulted in a single band of the expected length (1250bp) of *sk* genes. Lane1: DNA Marker 1kb (Thermo scientific SM0311), Lane2 and 3: PCR products of *skg88* and *skstab902* gene from genomic DNA. The corresponding bands were indicated by arrows. The sizes of the bands of DNA marker are illustrated on the right.

Fig. S4. Agarose gel (1%) electrophoresis of the restriction enzyme analysis of the recombinant vector pET26b-SKG_{88}. Lane 1: Digested pET26b-SKG_{88} by *Bst*EII, produced two bands with the approximate size of 1400 and 5100 bp. Lane 2: Digested pET26b-SKG_{88} by *Nde*I-*Xho*I, yielded 5230 and 1250 bp fragments corresponding to vector and PCR fragments, respectively. The corresponding bands were indicated by arrows. Lane 3: DNA Marker 1kb (Thermo scientific SM0311). The same analysis for the other two parental constructs pET26b-SK_{ALAB49} and pET26b-$SK_{STAB902}$ produced the same results (not shown).

Fig. S5. Analysis of the protein expression and purification by SDS/PAGE (12%). For protein expression, first the transformation of *E. coli* Rosetta cells (Novagen, USA) with the seven SK-encoding recombinant vectors (three parental vectors: pET26b-SK_{G88}, pET26b-SK_{ALAB49} and pET26b-$SK_{STAB902}$ and four domain-exchanged chimeric vectors: pET26b-SK_{C1} to pET26b-SK_{C4}) by standard $CaCl_2$ method was performed. Subsequently, protein

expression was induced at OD_{600} of 0.5–0.6 by isopropyl-β-D-thio-galactoside (IPTG) to a final concentration of 1 mM for 3 hours at 37°C. Finally, cells were harvested by centrifugation and stored at -20°C for purification steps. Purification of His-tagged SK proteins from induced *E.coli Rosetta* cells was performed under native conditions, using nickel-nitriloacetic acid (Ni-NTA) affinity chromatography and according to manufacturer's protocol (QIAexpressionist, 2002, Qiagen company website). Briefly, the cell pellets were resuspended in binding buffer (50 mM NaH_2PO_4, 300 mM NaCl, 10 mM imidazole) with 0.5 mg/ml lysozyme at 2–5 ml per gram wet weight. After incubation on ice for 30 min, the cells were disrupted by sonication, and supernatant was collected after centrifugation at 10,000 g for 20-30 min at 4°C. After addition of 1ml resin Ni-NTA to the clear lysate, the mixture was shaken at 4°C for 60 minutes, loaded on column and washed 4 times with 4 ml wash buffer (50 mM NaH_2PO_4, 300 mM NaCl, 20 mM imidazole) then 4 times with 0.5 ml elution buffer (50 mM NaH_2PO_4, 300 mM NaCl, 250 mM imidazole) (QIAexpressionist 2002). SDS-PAGE analyses were performed according to standard procedures [15]. (A) Analysis of the bacterial crude extracts for expression by pET26b-SK_{G88}. Lanes 1-3; un-induced bacterial cells, Lane 4; protein marker 10-180 kDa (SM7012 CinnaGen Co), Lanes 5-8; corresponds to IPTG induced cells with 0.3, 0.5, 0.7, 1 and 1.2 mM IPTG, respectively. (B) Analysis of protein purification steps for pET26b-SK_{G88}. Lanes 1- 4 represent the elution E1 to E4, respectively collected after protein extraction under native condition. Lane5: protein marker 10-180 kDa (SM7012 CinnaGen Co). Arrows indicate the location of 47 kDa (SK). Analysis of other constructs for expression and purification produced the same results (not shown).

Fig. S6. Confirmation of the expressed proteins by western blotting. Western blotting was performed according to the standard protocols [15]. Briefly, proteins were transferred from SDS-PAG to the nitrocellulose membrane and the membrane was blocked by 5% BSA. Mouse anti-His monoclonal antibody (Qiagen, USA) was used as the primary antibody and goat anti-mouse IgG conjugated to HRP (Horse Radish peroxidase) (Qiagen, USA) as the secondary (tracking) antibody. Detection of the bands was by 3, 3-diaminobenzidine (DAB) (Qiagen, USA). Western-blot analysis for $SK2a_{G88}$ and SK_{C1} proteins are shown. Lane 1; molecular weight marker (SM7012, Cinnagen Co), lanes 2 and 4; crude lysis of *E. coli* Rosetta cells after induction by IPTG (1mM), expressing $SK2a_{G88}$ and SK_{C1}, respectively, lane 3; crude lysis of *E. coli* Rosetta cells before induction (no band was observed). Lanes are spliced together to remove an intervening lane and the vertical dotted line is at the location of the spliced lanes. The arrow indicates the location of 47 kDa (SK).

Fig. S7. Calibration curve for standard SK. Serial dilutions of Streptase® (CSL, Behring, Germany), a commercially available standard SK, were used to prepare the standard calibration curve based on Hydrolysis of S-2251 by Pg, as explained in Fig. 2 and Fig. 3.

Fig. S8. Amino acid sequence alignment of SK proteins corresponding to reference strain SK_{9542} (*S. equisimilis*, ATCC9542, the commercial source for production of SK), $SK2b_{ALAB49}$, $SK2a_{G88}$, and $SK2a_{STAB902}$. The alignment was created using MEGA6 software [14]. Conserved (identical) amino acids in the alignment are indicated by dots. The exchanged fragments are highlighted.